

Threat learning by proxy: Semantic structures facilitate emotional memory integration  
throughout the MTL and medial prefrontal cortex

Samuel E Cooper<sup>1</sup>, Augustin C Hennings<sup>2</sup>, Sophia A Bibb<sup>3</sup>, Jarrod A Lewis-Peacock<sup>1,4,5,6</sup> &  
Joseph E Dunsmoor<sup>1,5,6</sup>

<sup>1</sup>Department of Psychiatry and Behavioral Sciences, University of Texas at Austin

<sup>2</sup>Princeton Neuroscience Institute, Princeton University

<sup>3</sup>Neuroscience Graduate Program, Ohio State University

<sup>4</sup>Department of Psychology, University of Texas at Austin

<sup>5</sup>Center for Learning and Memory, University of Texas at Austin

<sup>6</sup>Department of Neuroscience, University of Texas at Austin

Contacts: [samuel.cooper@austin.utexas.edu](mailto:samuel.cooper@austin.utexas.edu); [joseph.dunsmoor@austin.utexas.edu](mailto:joseph.dunsmoor@austin.utexas.edu)

Draft version 1.0 submitted for review 10/15/2023. This version of the paper has not been peer reviewed and will likely change during the review process. Supplemental materials are available at <https://osf.io/bpv97/>

## Abstract

Emotional experiences can profoundly impact our conceptual model of the world, modifying how we represent and remember a host of information even indirectly associated with that experience in the past. Yet, how a new emotional experience infiltrates and spreads across pre-existing semantic categories is unknown. We used an aversive sensory preconditioning paradigm in fMRI (N=35) to investigate whether threat memories integrate with a pre-established category to alter the representation of the entire category. We observed selective but transient changes in the representation of conceptually-related items in the amygdala, medial prefrontal cortex, and occipitotemporal cortex following threat conditioning to a simple cue (geometric shape) pre-associated with a different, but related, set of category exemplars. These representational changes persisted beyond 24-hours in the hippocampus and perirhinal cortex. During threat conditioning, reactivation of the semantic category interacted with hippocampal/medial prefrontal cortex activity to predict subsequent amygdala activity toward novel category members at test, providing evidence for online integration promoting threat generalization. Behaviorally, threat conditioning by proxy selectively and retroactively enhanced recognition memory, and increased the perceived typicality of the semantic category indirectly associated with threat. These findings detail a complex route through which new emotional learning generalizes by modifying associative networks built up over time and stored in memory as conceptual knowledge.

## Introduction

Imagine you developed a fear of dogs after a terrifying encounter at a relative's house. As time goes by, you realize that not only do you avoid your relative's dog, but parks, hiking trails, and certain friends' houses; all locations that did not previously cause anxiety, but where you know through experience that dogs might be off-leash. This illustrates the complex relationships humans draw on to integrate emotional experiences into pre-existing knowledge structures, allowing us to draw meaningful inferences about the possibility of danger in the absence of direct knowledge. This cognitive process conforms to long-standing principles from learning theory<sup>1</sup> and is operationalized by paradigms wherein stimulus representations are indirectly modified through reinforcement of related stimuli, known as higher-order conditioning<sup>2,3</sup>.

A flexible learning and memory system that can efficiently update prior stimulus representations and knowledge structures with new learning is clearly adaptive<sup>4</sup>; we can predict the potential for harm without having to experience the negative consequences directly (if you avoid parks, you lower even the minuscule possibility of getting bit by another dog). Conversely, an experience of threat that persistently and indiscriminately modifies an entire semantic network can facilitate maladaptive levels of heightened generalization to harmless stimuli or situations only tangentially related to the memory of threat (e.g., avoiding other commonly domesticated animals). This maladaptive form of generalization characteristic of many anxiety-related disorders, such as posttraumatic stress disorder (PTSD) and obsessive-compulsive disorder<sup>5-8</sup>. Although the ability to modify pre-existing knowledge structures, or schemas<sup>9</sup> with new learning is a hallmark of human cognition, the neurobehavioral mechanisms by which threat learning might do this are not well understood.

There have been at least two primary approaches for studying how a new experience updates our mental model of the world by modulating memories related to those experiences. One approach involves animal learning models that incorporate sensory preconditioning protocols. Sensory preconditioning is a long-standing task in which animals first learn an association between at least two arbitrary and affectively neutral stimuli (e.g., tone and light) in the absence of meaningful reinforcement (i.e., latent learning)<sup>2,10–13</sup>. Then, one of the stimuli is used as a conditioned stimulus (CS, the light) in a learning phase where it comes to predict a biologically salient unconditioned stimulus (US; e.g., a shock in threat conditioning). Finally, a transfer phase tests whether the preconditioned stimulus (PS, the tone) elicits a conditioned response (CR; e.g., freezing) similar to that elicited by the CS during the learning phase. Neurobiological research shows consistent involvement of the hippocampus, perirhinal cortex (PRC), and orbitofrontal cortex (OFC) at the different phases of learning and retrieval<sup>14</sup>. In aversive sensory preconditioning, the PRC cooperates with the basolateral amygdala (BLA) to coordinate indirect PS-US threat associations<sup>15,16</sup>. The other primary approach involves episodic memory tasks in humans that require novel inferences about pairs or groups of previously encoded stimuli based on new learning. The paradigms used in these studies include modified versions of sensory preconditioning<sup>4,17,18</sup>, as well as associative or transitive inference tasks<sup>19,20</sup>, and consistently show engagement of the hippocampus and medial prefrontal cortex (mPFC) for integrating across overlapping stimuli or events to draw novel inferences.

Integrating a memory of threat with broad semantic structures could lead to widespread changes in how object concepts are perceived, appraised, and remembered<sup>21,22</sup>. In this way, the transfer of emotional value could bypass direct instances of previously learned PS-CS pairings and spread merely through the underlying associative networks built up over time and stored in

memory as semantic knowledge. Using the earlier example, it is unnecessary to have prior experience with the vicious dog outside of your relative's house; pre-existing knowledge of where dogs are likely to be encountered is sufficient to motivate avoidance of those locations after the attack. Neuroimaging research shows that threat conditioning modulates cortical representations of object concepts that are directly associated with threat<sup>23–25</sup>. However, whether and how memory integration provides a route to *indirectly* implant emotional value into existing conceptual knowledge structures is unknown.

A major question concerns *when* integration occurs for events that overlap with previous experiences<sup>4,19,20,26</sup>. An online integration (i.e., integrative encoding, retrospective integration, or mediated learning) account proposes that the mental representation of the PS is reactivated on CS trials during conditioning, thereby integrating the PS and US representations at the time of reinforced learning<sup>16</sup>. Evidence from aversive sensory preconditioning tasks in rodents suggests that online integration requires the PRC, as temporary lesions of the PRC spare direct conditioning but prevent the transfer of conditioned learning to the PS<sup>14</sup>. Non-aversive memory integration tasks in humans likewise show that hippocampal activity at the time of learning predicts successful inference and preferences toward the paired preconditioned cues at test<sup>17</sup>; however, this effect is not always replicated<sup>27</sup>.

Alternatively, the retrieval account<sup>28</sup> emphasizes processes during the transfer test phase, whereby PS presentations elicit retrieval of the previously paired CS, which brings with it the representation of the US to inform behavior (i.e., chaining, or prospective integration) without a mediated PS-US representation. Appetitive sensory preconditioning work in rats<sup>29</sup> and in humans<sup>30</sup> suggests the OFC is required to retrieve indirectly acquired positive-value information of the PS to predict novel outcomes during retrieval.

These two accounts are not mutually exclusive. Dynamic behavioral demands might necessitate integration at the time of reinforced learning (conditioning) in some instances, or at retrieval (transfer test) in others<sup>28</sup>. For example, online integration at the time of emotional learning might modify internal representations of specific instances of the PS pre-associated with the CS in preparation for reencountering that specific PS<sup>16–18</sup>. Retrieval-based integration might rely on pattern completion processes, subserved by the hippocampus<sup>26</sup>, or relational reasoning, subserved by the hippocampus and mPFC<sup>19</sup>, to draw upon a broader network of relational links when encountering novel instances of the PS at test.

Here, we investigated the neurobehavioral mechanisms by which emotional learning indirectly modulates the representation of object concepts through memory integration. We used fMRI while participants completed a novel two-day sensory preconditioning task and applied multivariate pattern analysis (MVPA) to test different accounts for how regions in the medial temporal lobe (MTL) and mPFC facilitate integration of a threat memory with a previously associated semantic category. During preconditioning, trial-unique (non-repeating) exemplars from two semantic categories (animals or tools, counterbalanced between participants) served as PSs and were paired with a geometric shape (square or circle, also counterbalanced). Then, during threat conditioning, one of the shapes (CS+) predicted an aversive electrical shock, while the other shape was safe (CS-). Next, novel category exemplars from the PS categories (now referred to as PS+ and PS-, indirectly associated with the CS+ and CS-, respectively) were presented alone during two transfer tests, separated by a brief reminder of the CS-US association<sup>31</sup>. The next day, participants completed a second set of transfer tests in the scanner to assess whether representational changes persist over a 24-hour period. The experiment concluded with a

recognition memory test and subjective ratings of category typicality for the PSs encoded before and after threat conditioning on Day 1.

We predicted that aversive sensory preconditioning with trial-unique exemplars would be sufficient to generate a category-level association with the CS, which would then selectively modulate patterns of neural similarity for novel category members at test following direct CS-US learning. To investigate the mechanism underlying potential category-level modulation, we tracked neural reactivation of the PS+ category during conditioning on CS+ trials, which would putatively support the recombination of the PS category and the CS at the time of threat conditioning (online integration), as well as reinstatement of threat-specific CS+ neural patterns on PS+ trials at test (retrieval account).

## Method

Behavioral data and code are freely available at the OSF repository for this study (<https://osf.io/bpv97/>). Neuroimaging data is available at the NIMH Data Archive (<https://nda.nih.gov/>).

## Participants

We recruited 37 participants ( $M_{age} = 21.5$ ,  $SD_{age} = 3.07$ , 19 identified as women, one as nonbinary, 17 as men) from the local community to complete all measures. All participants completed standardized, structured clinical interviews<sup>32,33</sup> with a trained clinical psychologist or technician and were determined to be free of any psychopathology, neurological disorder, or interfering medical conditions. Two participants did not return for the second testing session; therefore, analyses were conducted on a final sample of  $N = 35$ .

## Stimuli

For PSs, we used 180 non-repeating images of either animals ( $N = 90$ ) or tools ( $N = 90$ ) against a white background obtained from [www.lifeonwhite.com](http://www.lifeonwhite.com) or publicly available online resources and used in prior studies from our group. Each PS used in the experiment across all phases was a different basic-level exemplar (e.g., there were not two different pictures of a dog). We did not include typically threatening or phobia-related stimuli (e.g., spiders, snakes, knives). CSs were either an image of an orange square or a blue circle against a white background. Both shapes shared the same width, height, and luminance and were approximately the same size as the category exemplar images. Stimulus presentation was controlled by Psychopy<sup>34</sup>.

The US was a 5-ms electrical shock, delivered to the to the left index and middle finger. Shock intensity was determined through a brief calibration sequence prior to the experiment, in which participants reached a level described as “highly annoying and unpleasant, but not painful” (5-6 out of 10-point scale) through a stepwise procedure<sup>35</sup>. The shock was controlled using the STMEPM-MRI stimulation system from BIOPAC Systems (Goleta, CA).

### **Task and Procedures**

The current task, based on similar human work and optimized for MVPA<sup>36</sup>, consisted of seven phases across two days (see Fig. 1B). Day 1 consisted of a perceptual localizer, preconditioning, threat conditioning, and two immediate transfer tests. After shock and skin conductance response (SCR) electrodes were attached, participants completed the perceptual localizer (described below) and then a preconditioning phase in which a PS stimulus was presented for 4-6s, followed immediately by a CS presented for .5s. Participants were instructed prior to the task that their goal is to learn which category is associated with each shape, and that they will need to remember this association. PS category (PS+ and PS-) and CS shape (CS+ and CS-) pairings were counterbalanced across participants. For each PS presentation during preconditioning (30



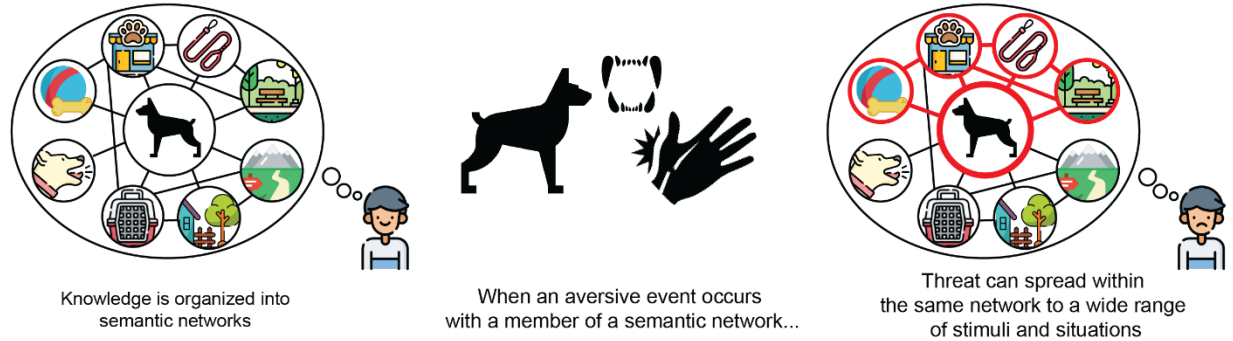
animals, 30 tools), participants indicated which shape they thought would next appear using a 4-item scale (“Definitely square”, “Maybe square”, “Maybe circle”, “Definitely circle”). After this phase, participants received instructions that they were now at risk for shock and received a single reminder shock during a blank screen to ensure the perceived intensity had not changed. Next, participants completed the threat conditioning phase, in which only CSs were presented and one CS co-terminated with shock (CS+, 12 trials, 66% reinforcement) and one was never paired with shock (CS-, 12 trials); this was counterbalanced across participants. CSs were presented for 5-7s. PSs were not presented during this phase. Participants provided shock expectancy ratings for each CS, again using a 4-item scale (“Definitely shock”, “maybe shock”, “maybe no shock”, “definitely no shock”). Threat conditioning was immediately followed by the two transfer tests. In these tests, participants again viewed PSs from each category (30 animals and 30 tools; 15 of each category in each test) for 4-6s and continued to provide shock expectancy ratings as they did during the threat conditioning phase. No US was ever administered following a PS. Between the two transfer tests there was a seamless presentation of two reinforced CS+ trials that were used as “booster trials” to remind participants of the CS-US association<sup>31</sup>. We refer to these transfer tests as immediate Transfer 1 and Transfer 2 throughout this report.

On Day 2, approximately 24-hours later, participants completed identical transfer tests as on Day 1 (including the two reminder CS-US trials in between the tests). We refer to these tests as 24-hour Transfer 3 and 4. Critically, the exemplars presented on Day 2 were also novel category members and not seen on Day 1. Intertrial intervals (ITI) were jittered (5-9s) for all phases across both days.

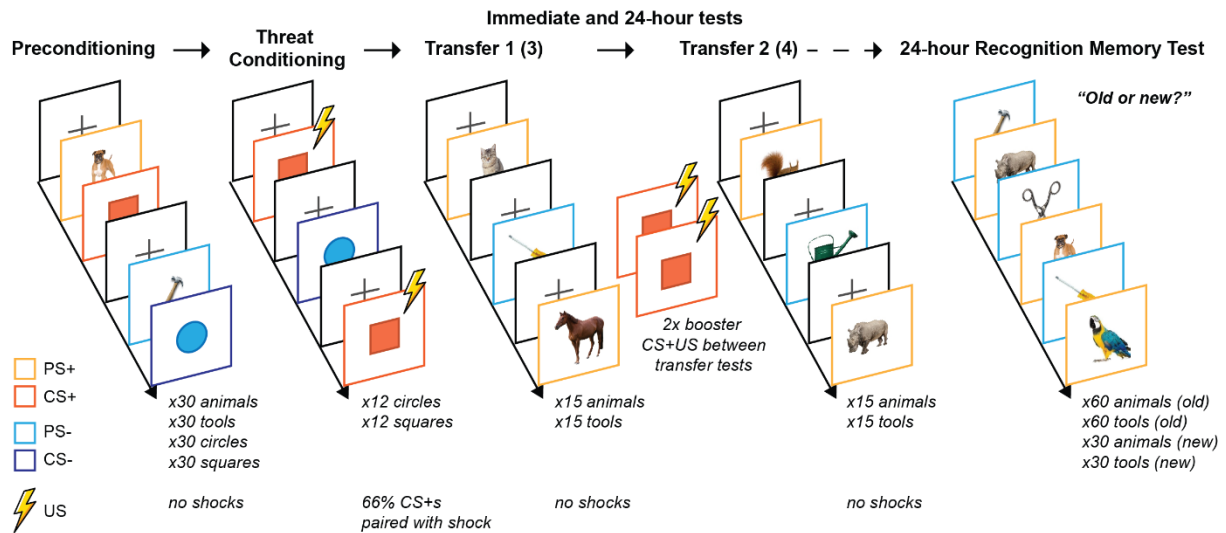
Finally, participants completed a recognition memory test, in which they viewed all Day 1 category stimuli (120 in total) in addition to foil stimuli (30 novel tools, 30 novel animals). We

explicitly informed participants that only Day 1 or new stimuli would be presented and that no Day 2 stimuli were presented. Image order was pseudo-randomized and balanced such that participants viewed an equal number of items from each category in each third of the phase. Each image was presented for 3s and prompted participants to provide a response on a 4-item scale (“definitely new”, “maybe new”, “maybe old”, “definitely old”). Once out of the scanner, participants viewed each Day 1 category stimulus on a separate computer. They viewed each image one at a time and provided a 1-7 typicality rating for each (1 = not typical at all of its category; to 7 = very typical of its category). Typicality rating trials were self-paced.

### A Threat can generalize across higher-order semantic pathways



### B Indirectly integrating threat into a semantic network using sensory preconditioning



### C

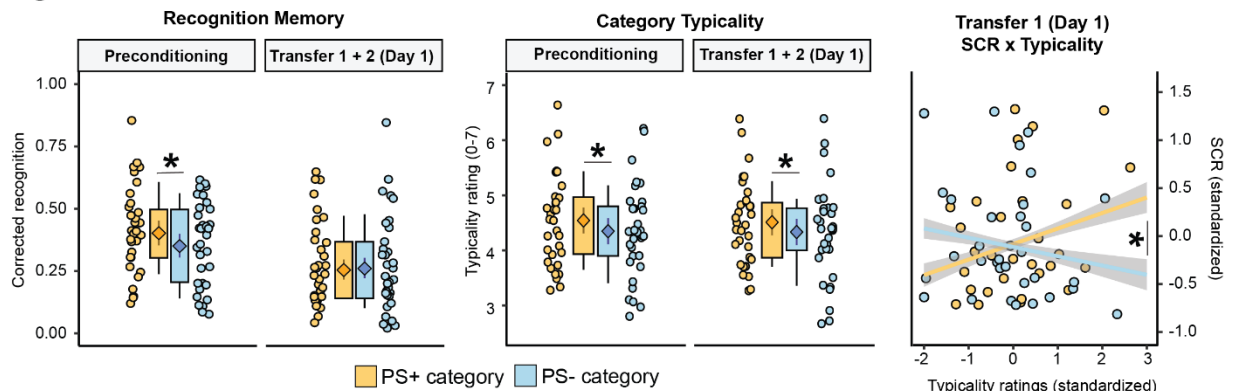


Fig 1. (A) Schematic overview. Threat associations can generalize from a single traumatic incident (e.g., a car crash) across a related semantic network (e.g., things related to cars, such as roads, car keys, or garages), even when related stimuli were not present nor perceptually resemble aspects of the traumatic incident.

(B) 2-day sensory preconditioning task structure. Semantic categories were paired with one of two neutral shapes. One of these shapes (CS+) was then paired with the US during threat conditioning; the semantic category paired with this shape is labeled the PS+, the other shape and category are CS- and PS-, respectively.

(C) Behavioral results. A retroactive bias towards increased memory for PS+ (vs. PS-) items encoding during precondition is behavioral evidence for successful mediated learning. Further evidence includes increased reported mean typicality for PS+ (vs. PS-) items and an immediate Transfer 1 x SCR interaction, such that higher reported mean typicality for the PS+ category was associated with increased SCR to PS+s during transfer. Box-and-whisker plots represent the middle 50% (25<sup>th</sup> – 75<sup>th</sup> percentile) of the plotted individual data points (fitted values; for recognition data values are transformed back to the response scale) in the box, with the whiskers showing the s.e.m. Inside the box, the point and error bars represent the mixed effects regression estimated marginal mean and 95% confidence intervals. Error bars account for random effects structure.

CS+ = conditioned threat cue; CS- = conditioned safety cue; PS+ = preconditioned threat cue; PS- = preconditioned safety cue; SCR = skin conductance response;; Transfer 1 = transfer test phase prior to reminder CS/US presentations; Transfer 2 = transfer test phase immediately following reminder CS/US presentations; US = unconditioned stimulus.

\*  $p < .05$

## **Skin Conductance Response**

SCRs were acquired from the hypothenar eminence of the left palmar surface using disposable pre-gelled snap electrodes connected to the MP-160 BIOPAC System (BIOPAC Systems). In line with previously described procedures<sup>37,38</sup>, an SCR was considered related to CS or PS presentation if the trough-to-peak deflection occurred 0.5–3s following stimulus onset, lasted between 0.5 and 5.0s, and was greater than 0.02 microsiemens ( $\mu$ S). We scored responses that did not fit these criteria as a zero. We obtained SCR values using a custom MATLAB (The Mathworks Inc., Natick, MA) script that extracts SCRs for each trial using the above criteria<sup>39</sup>. Raw SCR scores were square root transformed prior to statistical analysis to normalize the distribution<sup>40</sup>. We did not exclude participants based on performance-based rules, per best practices<sup>41</sup>.

## **Functional MRI Acquisition**

Scanning was completed using a Siemens Vida 3T MRI scanner at the University of Texas at Austin with the support of the Biomedical Imaging Center (RRID:SCR\_021898). We acquired functional data with a 64-channel head coil at 2.5mm isotropic resolution. Using the scanner software, we automatically oriented slices parallel to the anterior-posterior commissure. We measured BOLD using T2\* EPI sequences (TR = 1000ms, TE = 86ms, FOV = 86 x 86, multiband acceleration factor = 6). Before each functional series, we collected T2\* field maps with opposite encoding phase to assist with distortion correction during preprocessing. We also collected

anatomical images to assist in image registration: a T1w anatomical image (MPRAGE, .8mm isotropic) was collected during each session, and one T2w anatomical image (.8mm isotropic) was collected on Day 2.

### **Image Preprocessing**

We used the fMRIPrep 20.2.6 toolbox<sup>42</sup> to conduct primary preprocessing of MRI data. This toolbox generates a reproducible workflow of preprocessing steps, which is documented in full in the Supplementary Materials. In brief, functional images were registered to the MNI template and resampled to 2mm isotropic space. After this initial registration, no additional 3D transformations were applied to the images. Basic functional preprocessing included skull stripping, grey matter parcellation via FreeSurfer<sup>43</sup>, and susceptibility distortion correction using the collected field maps. fMRIPrep produced a series of estimated confound signals, which were included in all general linear model (GLM) estimations to remove these confounds from the images. These confounds included the first principal component of estimated physiological noise, framewise displacement, six standard head motion parameters, and the discrete cosine-basis regressors calculated by fMRIPrep for the purpose of high-pass filtering.

### **General Linear Models and Whole-Brain Analyses**

All GLMs were computed using the *nilearn* 0.9.2 package<sup>44</sup> in Python 3.8.1, with standard boxcar modeling of trials convolved with a Glover hemodynamic response function and a lag-1 autoregressive model to account for serial correlations. For standard GLM univariate analyses, we included separate regressors for each stimulus across all trials of a given phase (e.g., PS+ and PS- in a transfer phase) and applied smoothing with a Gaussian kernel (FWHM = 6mm). All images were masked to only include likely grey matter voxels (MNI152 template, thresholded at 20% grey matter probability). We also generated Least Squares-Separate (LSS) style betaseries images for

all phases<sup>45,46</sup>, in which we iteratively estimated activity for a given trial in each phase while also including all other trials from the same category in the same phase as regressors of no interest. No spatial smoothing was applied to LSS betaseries images to facilitate MVPA.

Whole-brain statistical analyses were conducted using AFNI 22.3.04<sup>47</sup> and a family-wise error approach. Two-tailed t-tests were conducted on each voxel within participant-level whole-brain maps using 3dttest++ (with -Clustsim option). Significant cluster size was determined via  $k = 10,000$  random permutations of null t-test results, which were then run through 3dClustSim to identify cluster-thresholds for each  $p$ -value. Using these cluster-thresholds, 3dClusterize was used to identify clusters in group-level masks and extract cluster statistics (significant at cluster  $p < .05$ , voxel  $p < .001$ , third-nearest neighbor clustering).

## ROI Selection

ROIs were chosen in accordance with *a priori* hypotheses based on extensive rodent preconditioning work<sup>14</sup> and human neuroimaging of threat conditioning<sup>48,49</sup>. At the group-level, bilateral BLA were defined using the Julich probabilistic atlas<sup>50</sup>, whereas bilateral perirhinal cortex was extracted from a probabilistic map of manually segmented hippocampal and parahippocampus subregions<sup>51</sup>. All probabilistic maps but the BLA were thresholded at 50% or greater likelihood of a given voxel belonging to that anatomical region. The BLA map used a more stringent threshold of 75% due to increased noise in this region and to increase the chance voxels from anatomically adjacent amygdala subregions were not included in the BLA mask. For the medial PFC, as well as full amygdala and hippocampus ROIs, we defined ROIs for each participant anatomically using the relevant FreeSurfer parcellations of the Desikan-Killiany atlas.

## Perceptual Localizer

Participants viewed images from categories that included animals, tools, shapes, and phase-scrambled animals and tools. Each image was shown for 1s and separated by 1s. Participants were given an irrelevant task (identifying a single repeated image with a button press, i.e., perceptual N-back) to keep their attention during the localizer. Images were presented in two runs. Each run included four blocks that consisted of 8 images each. Each category was presented for two blocks each (total 16 images per category). There were 16s of rest between each block. Each image was distinct from any other localizer images and from stimuli used during experimental phases. LSS betaseries for each localizer block were computed.

### **Multivariate Pattern Analysis**

MVPA included representational similarity analyses (RSA) and multivariate decoding. For RSA, we applied the *nilearn* library and custom Python code to LSS betaseries for trial-by-trial data from each phase and each stimulus (weighted by mean univariate estimates from the same phase and stimulus type to reduce noise<sup>52-54</sup>) to create a representational similarity matrix for each *a priori* ROI. In these matrices, each cell is a Pearson-correlation between all pairs of PS+ and PS- images across all phases. We then Fisher-z transformed matrices and extracted the mean value of the cells that corresponded to within-category similarity (e.g., all cells with PS+ to PS+ correlations). We also extracted the mean value for the cells that corresponded to the similarity of each transfer phase to either threat conditioning or preconditioning for each stimulus type (e.g., all cells with correlations between PS+s in generalization and CS+s in threat conditioning or in preconditioning). We refer to these two types of RSA as within-category similarity and across-phase similarity, with within-category similarity an index of neural similarity for items from the same category that were encoded in the same phase, whereas

across-phase similarity indexes neural similarity of items that were encoded in separate phases of the experiment.

Classification was conducted using the *scikit-learn* library<sup>55</sup> and custom Python scripts. In line with similar prior work<sup>23,24</sup> and knowledge on canonical object regions<sup>56</sup>, we focused classification on occipital and temporal regions with voxels that uniquely code for animals or tool object categories. These category-selective cortices were functionally identified at the group-level through whole-brain analyses (voxel-wise  $p \leq .001$ , cluster corrected  $p < .05$ , see Supplementary Table S1 and Fig. S2) of univariate animal > tool and tool > animal contrasts of perceptual localizer fMRI data. For each set of contrasts, a 5mm sphere was drawn around the peak intensity voxel to focus analyses on the most selective voxels and to ensure a similar number of features (voxels) were submitted to classification for each category (animal cortex = 64 voxels, tool cortex = 72 voxels). We then trained an L2 weighted logistic regression classifier (“liblinear” solver) to decode category-specific activity (with animals, tools, and scrambled images submitted to classification) in localizer functional data in each of the two identified ROIs. We assessed classifier sensitivity by cross-validating performance from one localizer run with the other for each classifier (mean animal cortex ROC area under the curve [AUC] = 67.5%, SD = 10%; mean tool cortex ROC AUC 70.5%, SD = 13.2%). Three participants were removed from further analyses due to unreliable classification (individual AUC values < 0.5), resulting in N = 32 for analyses involving decoding data.

### **Statistical Analyses**

All ROI and behavioral group-level statistical analyses were conducted using R 4.3<sup>57</sup>. We used robust linear mixed effects regression for all analyses, which is consistent with current recommendations for task-based fMRI data with multiple repeated factors<sup>58–60</sup>. All models were



specified using the `robustlmm`<sup>61</sup> and `lme4`<sup>62</sup> libraries, which reduces bias in clustered (repeated-measures) data by minimizing the influence of extreme outlier observations<sup>60</sup>. Unless otherwise noted, we included a participant random effect with task phase nested within participant as a random slope to limit the number of separate models we constructed and tested (see Supplementary Materials for full model details). From this initial model, we then tested the difference in stimuli estimated marginal means (using the *emmeans*<sup>63</sup> library) within each phase (e.g., PS+ vs. PS- during each transfer test). Per recommendations, all models were fit with restricted maximum likelihood (REML), and degrees of freedom were generated with the Kenward-Rogers method<sup>64,65</sup>. We provide standardized betas, Wald *t*-values (*t<sub>wald</sub>*), *p*-values, and parametric 95% confidence intervals for all tests unless otherwise noted<sup>66</sup>. For recognition memory data, a generalized linear mixed-effects model (binomial/logistic) was used to analyze dummy-coded high-confidence recognition responses (0 = “sure new”, 1 = “sure old”), with between-subject mean false alarm rate modeled as fixed-effect covariates to disambiguate within- and between-subject effects<sup>67–69</sup>. Asymptotic *z*-tests (*z<sub>asyp.</sub>*) were conducted for these models<sup>70</sup>. One participant reported falling asleep during recognition runs and was therefore excluded from analysis of these data (N = 34). For Day 2 behavioral tests, we combined immediate Transfer 1 and Transfer 2 stimuli for all analyses. For behavioral tests involving PS data (i.e., data with trial-unique stimuli), we modeled data at the trial-level with trial random and fixed effects to account for additional observations and restrict our degrees-of-freedom<sup>65,71</sup>.

## Results

### Behavioral results

**Threat conditioning.** Confirming successful differential threat acquisition, mean SCRs were greater for the CS+ relative to the CS-,  $\beta = .45$ ,  $t_{wald}(34) = 4.97$ ,  $p < .001$ , 95%CI [.26, .63],

as were mean shock expectancy ratings,  $\beta = 2.16$ ,  $t_{wald}(33.5) = 41.18$ ,  $p < .001$ , 95%CI [2.05, 2.26]. See Fig. S1 in Supplementary Materials for plotted results.

**Transfer tests.** Mean SCRs were not significantly different between the PS+ and PS- during the immediate (Day 1) or 24-hour (Day 2) transfer test ( $ps \geq .085$ ). Given prior evidence that typicality influences category-level threat generalization<sup>72</sup>, we tested whether individual differences in participants' mean typicality for the PS+ category predicted arousal toward PS+ items at test. During the initial transfer phase (Transfer 1) immediately after conditioning, category typicality significantly positively moderated the relationship between stimulus and SCRs,  $\beta = .117$ ,  $t_{wald}(1490) = 1.99$ ,  $p = .046$ , 95%CI [.01, .23] (Fig. 1C). Importantly, this association between retrospective typicality ratings and within-session arousal was selective to the PS+ category. Typicality was not a significant moderator in other experimental phases ( $ps \geq .376$ ). This result shows that aversive sensory preconditioning increased physiological arousal in participants who viewed these items as more representative of the category.

Participants did not report elevated shock expectancy ratings during the transfer tests. Using a 4-AFC shock expectancy scale, mean expectancy ratings indicated an overall low likelihood of receiving a shock on either PS+ (Day 1:  $M = 1.175$ ; Day 2:  $M = 1.045$ ) or PS- (Day 1:  $M = 1.45$ ; Day 2:  $M = 1.14$ ) trials. Interestingly, ratings were nominally enhanced on PS- trials during immediate Transfer 1 and 24-hour Transfer 3 (Transfer 1:  $\beta = -.227$ ,  $t_{wald}(1950) = -4.987$ ,  $p < .001$ , 95%CI [-.31, -.13]; Transfer 3:  $\beta = -.152$ ,  $t_{wald}(1943) = -3.035$ ,  $p = .002$ , 95%CI [-.24, -.05]); there was no PS+ vs PS- difference on either immediate Transfer 2 or 24-hour Transfer 4 (Transfer 2:  $\beta = .011$ ,  $t_{wald}(1950) = 0.248$ ,  $p = .803$ , 95%CI [-.078, .10]; Transfer 4:  $\beta < .001$ ,  $t_{wald}(1942) = -0.001$ ,  $p = .999$ , 95%CI [-.09, .09]). However, the ratings on PS- trials indicated a low likelihood of expecting shock. These results indicate that participants did not explicitly infer

that the PS category predicted threat at the level of subjective reporting. Assessing the relationship between expectancy and typicality ratings was challenged by overall low expectancy ratings and lack of variability in expectancy using the 4-AFC.

***Threat conditioning retroactively enhances memory for items pre-associated with a conditioned stimulus.*** Twenty-four hour corrected recognition memory performance was significantly greater for PS+ versus PS- items encoded prior to conditioning,  $\beta = 0.226$ ,  $z_{asympt.} = 2.28$ ,  $p = .022$ , 95%CI [.03, .42] (see Fig. 1C). There was no significant difference between PS+ and PS- items encoded during transfer test, immediately following conditioning,  $\beta = -.032$ ,  $z_{asympt.} = -0.299$ ,  $p = .765$ , 95%CI [-.24, .18].

***Subjective typicality ratings.*** Participants rated PS+ items as overall more typical of their semantic category, as compared to respective mean typicality ratings for the PS- category. This included items encoded during preconditioning,  $\beta = .10$ ,  $t_{wald}(3826) = 2.55$ ,  $p = .010$ , 95%CI [.01, .18], and the Day 1 transfer tests (Transfer 1 and 2),  $\beta = .09$ ,  $t_{wald}(3826) = 2.32$ ,  $p = .020$ , 95%CI [.02, .18] (see Fig. 1C). Follow-up tests did not reveal significant differences in typicality ratings for items encoded at preconditioning vs. transfer for either PS+,  $\beta = .01$ ,  $t_{wald}(126) = 0.41$ ,  $p = .681$ , 95%CI [-.06, .11], or PS- stimuli,  $\beta = .008$ ,  $t_{wald}(126) = 0.19$ ,  $p = .848$ , 95%CI [-.07, .09]. This result suggests that threat-conditioning retroactively and proactively enhanced subjective stimulus typicality, in line with prior findings<sup>73</sup>.

### **Univariate analysis of aversive sensory preconditioning**

***Whole-brain analyses.*** Univariate whole-brain fMRI analysis (voxel-wise  $p \leq .001$ , cluster corrected  $p < .05$ ) of the CS+ > CS- contrast for threat conditioning found significant clusters consistent with prior meta-analyses<sup>48</sup>, including the insula, thalamus, anterior cingulate, and striatum (see Supplementary Table S2, Fig. S3). We did not find significant whole-brain clusters

for the PS+ > PS- or PS- > PS+ univariate contrasts during the transfer phases on either day or during preconditioning.

**Univariate ROI analyses.** Activity in the BLA,  $\beta = 0.31$ ,  $t_{wald}(170) = 2.49$ ,  $p = .013$ , 95%CI [.06, .56], and hippocampus,  $\beta = 0.32$ ,  $t_{wald}(170) = 2.25$ ,  $p = .025$ , 95%CI [.04, .64], was significantly higher for the PS+ compared with the PS- during the immediate Transfer 1 test. Across all ROIs, there were no other significant PS+>PS- or PS->PS+ activations during the transfer tests ( $ps \geq .075$ ).

### Pattern similarity analysis of aversive sensory preconditioning

To examine potential modulation of category-level representations resulting from indirect threat learning, multivariate patterns of activation to each trial-unique PS item were correlated with the patterns from all other PS category exemplars encoded within the same experimental phase. As expected, there was no delineation in pattern similarity between the PS+ and PS- categories at pre-conditioning in any *a priori* ROIs ( $ps \geq .071$ ; Figure 2C and Figure 3), providing benchmark evidence that semantic categories were not differentially represented in multi-voxel patterns of activity prior to conditioning.

Following conditioning, category-selective occipitotemporal regions (identified from the independent category localizer) exhibited enhanced pattern similarity amongst items from the PS+ versus PS- category during Day 1 transfer tests (Transfer 1:  $\beta = 0.33$ ,  $t_{wald}(170) = 2.11$ ,  $p = .036$ , 95%CI [.02, .64]; Transfer 2:  $\beta = 0.35$ ,  $t_{wald}(170) = 2.28$ ,  $p = .023$ , 95%CI [.04, .66]) (see Fig. 2C). Notably, selectivity in pattern similarity between the PS+ vs. PS- categories was absent in category-selective visual regions after ~24-hours (Transfer 3:  $\beta = -0.02$ ,  $t_{wald}(170) = -0.15$ ,  $p = .877$ , 95%CI [-.33, .28]; Transfer 4:  $\beta = 0.07$ ,  $t_{wald}(170) = 0.46$ ,  $p = .642$ , 95%CI [-.23, .38]).

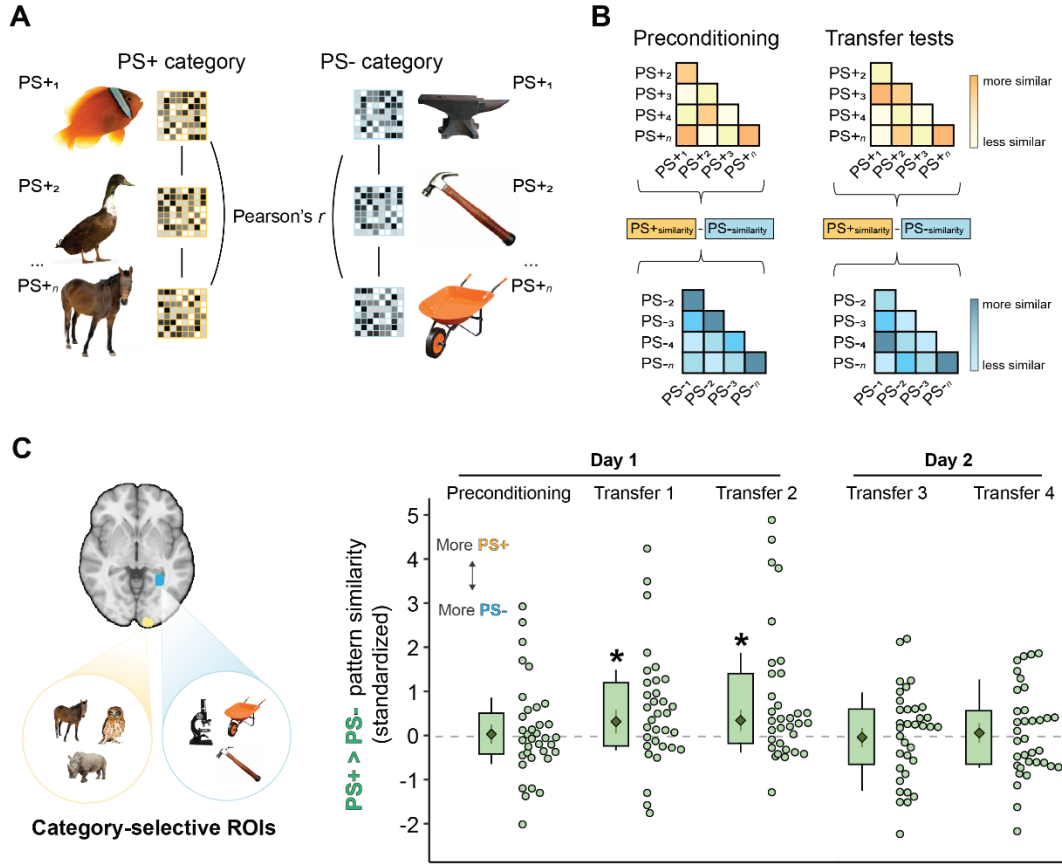


Fig 2. (A) Overview of within-category representational similarity analyses. Each multivoxel pattern for each stimulus is correlated with all other stimuli from the same category for all possible pairs.

(B) Correlations from within each category are averaged to form an overall metric of within-category similarity. PS+ and PS- similarity are compared within linear mixed models.

(C) Within-category similarity results for category-selective regions across all task phases. Data is represented as PS+ > PS- difference scores for visualization purposes only; all models and estimated marginal means incorporate separate PS+ and PS- values. Box-and-whisker plots represent the middle 50% (25<sup>th</sup> – 75<sup>th</sup> percentile) of the plotted individual data points in the box, with the whiskers showing the s.e.m. Inside the box, the point and error bars represent the mixed effects regression estimated marginal mean and 95% confidence intervals. Error bars account for random effects structure.

PS+ = preconditioned threat cue; PS- = preconditioned safety cue.

\*  $p < .05$

Across *a priori* ROIs from the medial temporal lobe and medial PFC (Figure 3), there was enhanced pattern similarity for trial-unique items from the PS+ versus PS- category in the PRC at both immediate transfer tests (Transfer 1:  $\beta = 0.29$ ,  $t_{wald}(170) = 3.05$ ,  $p = .002$ , 95%CI [.10, .48]; Transfer 2:  $\beta = 0.40$ ,  $t_{wald}(170) = 4.14$ ,  $p < .001$ , 95%CI [.21, .59]). This selectivity in PS+ pattern similarity in the PRC extended to the 24-hour test (Transfer 3:  $\beta = 0.33$ ,  $t_{wald}(170) = 2.93$ ,  $p < .001$ ,

95%CI [.14, .53]). In the hippocampus, enhanced pattern similarity was observed during the second transfer test on Day 1 ( $\beta = 0.18$ ,  $t_{wald}(170) = 2.16$ ,  $p = .031$ , 95%CI [.01, .34]) and extended to the first transfer test on Day 2 ( $\beta = 0.24$ ,  $t_{wald}(170) = 2.93$ ,  $p = .003$ , 95%CI [.08, .41]). The amygdala ( $\beta = 0.30$ ,  $t_{wald}(170) = 3.29$ ,  $p = .001$ , 95%CI [.12, .48]) and medial PFC ( $\beta = 0.34$ ,  $t_{wald}(170) = 3.01$ ,  $p = .003$ , 95%CI [.11, .57]) exhibited selectively enhanced PS+ pattern similarity during the second transfer test on Day 1, however, this selectivity did not extend to Day 2 in either region ( $ps \geq .059$ ).

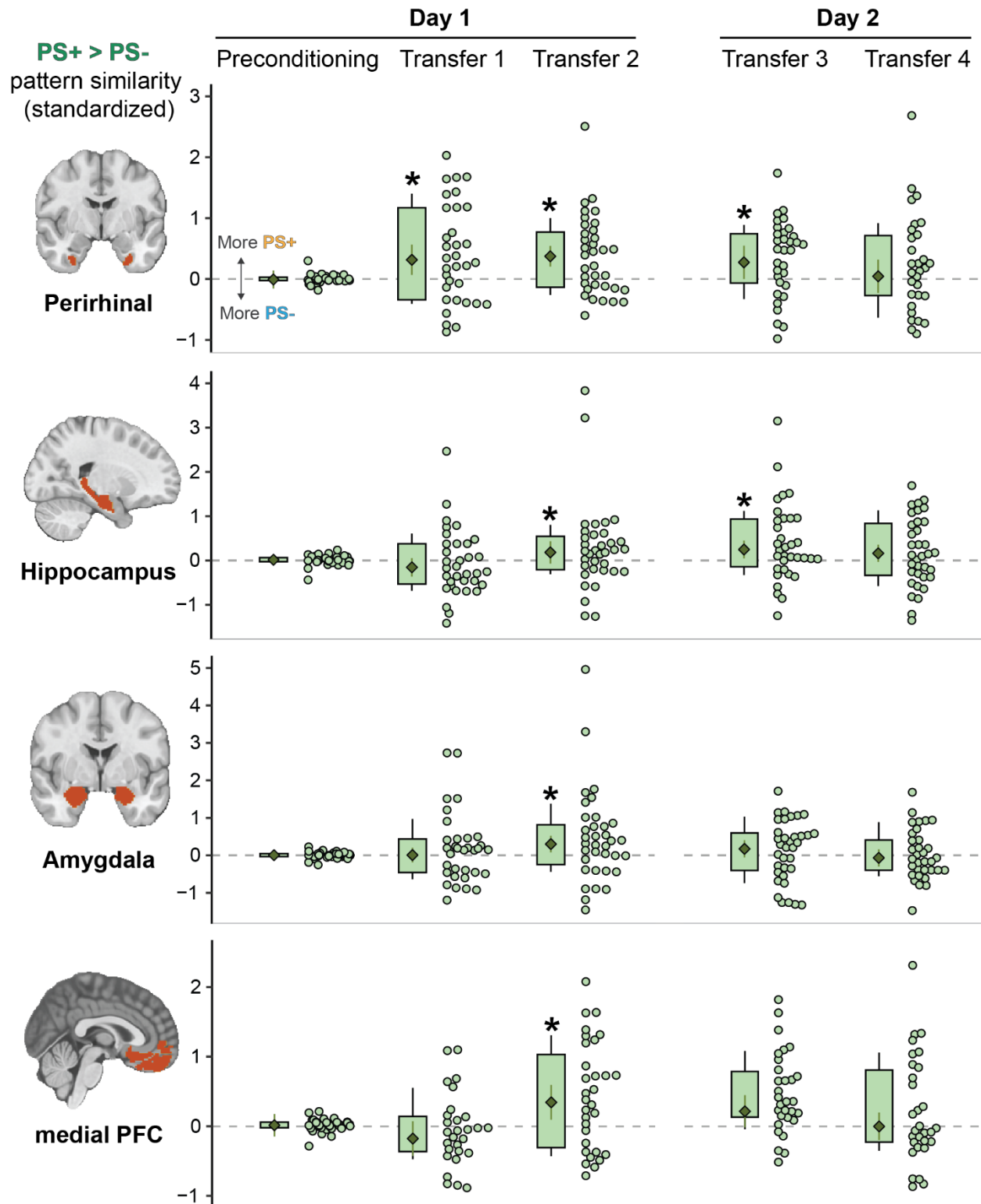


Fig 3. Within-category similarity across *a priori* anatomical ROIs. Perirhinal cortex and hippocampus showed increased PS+ similarity at immediate and 24-hour transfer tests, whereas the amygdala and medial PFC only showed this effect at the immediate transfer test. Data is represented as PS+ > PS- difference scores for visualization purposes only; all models and estimated marginal means incorporate separate PS+ and PS- values. Box-and-whisker plots

represent the middle 50% (25<sup>th</sup> – 75<sup>th</sup> percentile) of the plotted individual data points in the box, with the whiskers showing the s.e.m. Inside the box, the point and error bars represent the mixed effects regression estimated marginal mean and 95% confidence intervals. Error bars account for random effects structure.

PFC = prefrontal cortex; PS+ = preconditioned threat cue; PS- = preconditioned safety cue.

\*  $p < .05$

### **Threat pattern reinstatement during transfer tests**

Multivariate analyses have identified the amygdala and mPFC as reflecting neural threat patterns at tests of threat memory retrieval<sup>53,74,75</sup>. Here, we tested the degree to which multi-voxel threat patterns are reinstated during transfer tests. Multi-voxel activity patterns evoked by CS's trials during conditioning were correlated with their corresponding pre-associated PSs during transfer as a form of encoding-retrieval similarity<sup>53,76,77</sup>. There was significant reinstatement of CS+ threat conditioning neural patterns in the amygdala during the early transfer test (Transfer 1) on PS+ trials, as compared to corresponding CS-/PS- trials,  $\beta = 0.26$ ,  $t_{wald}(306) = 3.04$ ,  $p = .002$ , 95%CI [.09, .44] (see Fig. 4). Threat-specific pattern reinstatement was selective to the first transfer test (other transfer tests,  $ps \geq .816$ ). Interestingly, selective threat pattern reinstatement in the mPFC was observed in the second transfer test on Day 1,  $\beta = 0.36$ ,  $t_{wald}(306) = 4.72$ ,  $p < .001$ , 95%CI [.21, .52]. All other mPFC comparisons, as well as the same tests within PRC, hippocampus, and category-selective visual regions, were nonsignificant ( $ps \geq .088$ ).



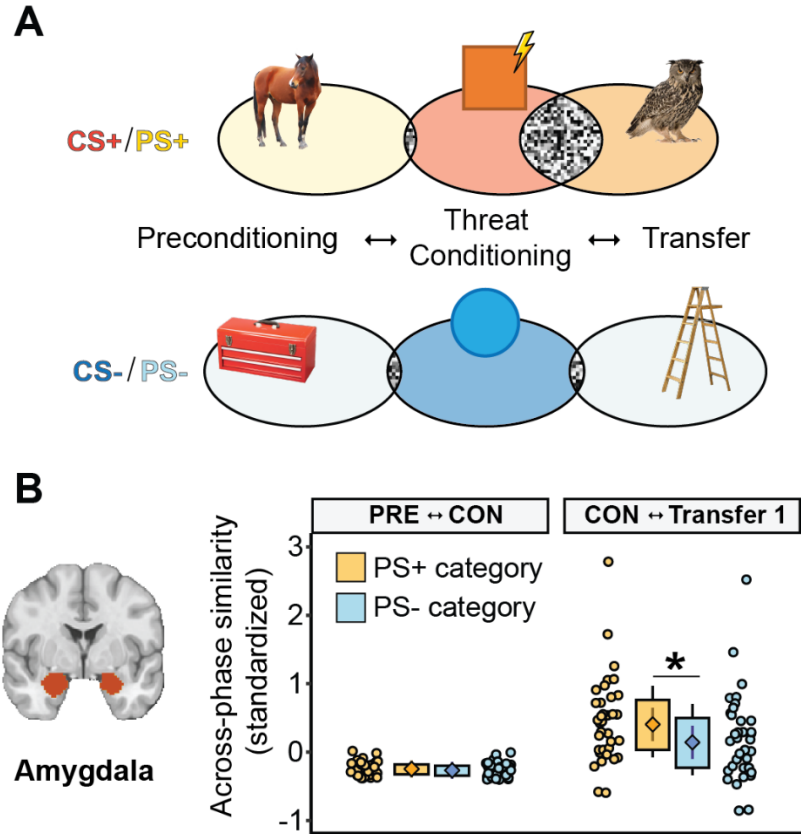


Fig 4. Across-phase neural similarity. Box-and-whisker plots represent the middle 50% (25<sup>th</sup> – 75<sup>th</sup> percentile) of the plotted individual data points in the box, with the whiskers showing the s.e.m. Inside the box, the point and error bars represent the mixed effects regression estimated marginal mean and 95% confidence intervals. Error bars account for random effects structure.

CON = threat conditioning; PRE = preconditioning; PS+ = preconditioned threat cue; PS- = preconditioned safety cue.

\*  $p < .05$

### Evidence of online integration through cortical reactivation during aversive learning

Using our validated classifier, we estimated reactivation of the PS+ category (animals or tools, counterbalanced) during the presentation of the CS+ at the time of threat conditioning in category-selective cortices as an index of online emotional memory integration. According to the online integration account, CS trials will trigger reactivation of the PS representation, which will undergo modification as CS-US learning progresses throughout conditioning, thereby resulting in a modified PS representation at test<sup>28</sup>. Decoded PS- category reinstatement on CS- trials served as a comparison condition. For all analyses, decoded category reactivation is referred to by PS+ or

PS- label, as for some participants the animal category was the PS+ and tool was PS-, and for others vice-versa. Decoding yields classifier evidence values (probability estimates), with larger values indicative of greater likelihood of reactivation. As expected based on related prior work<sup>52</sup>, classifier evidence for PS+ category reactivation was well distributed ( $M = .46$ ,  $SD = .15$ ,  $IQR = .22$ ) and significantly differed from zero (one-sample  $t$ -test,  $t(33) = 16.8$ ,  $p < .001$ ) (Figure 5B). Evidence did not significantly differ based on which category was the PS+ or PS- per participant,  $t(30) = -0.045$ ,  $p = .964$ . Similar results were found for the PS- category.

We then used individual participants' classifier evidence for the decoded PS+ (and PS-) on CS+ trials during conditioning to predict their degree of BLA activity during the transfer test on PS+ trials. The BLA was the key focus of this analysis, given its presumed role in retrieving the modified association of the PS+, which was indirectly altered at the time of threat conditioning (online integration) through reactivation of the PS+ representation<sup>16</sup>. To test for moderation of this relationship, we expanded the interaction with another term in two analyses: one with hippocampus univariate activity to CSs during threat conditioning, the other with mPFC activity to CSs during threat conditioning. We focused on these two regions due to their prominence in the memory literature as key hubs for episodic memory integration<sup>19</sup>. To determine if the addition of a separate hippocampus or mPFC univariate activity term to the interaction significantly improved model fit (a requirement for formal moderation analyses), we conducted likelihood ratio tests comparing models with and without the expanded interaction (Chi-square distribution, significance at  $p < .05$ ). All models continued to include the repeated-measures stimulus term (CS+/PS+/ CS-/PS-).

Reactivation of the PSs during CS trials did not selectively predict BLA activity during either transfer phase. However, interacting PS reactivation with CS univariate activity in

hippocampus,  $\chi^2(3) = 12.723, p = .005$ , or mPFC,  $\chi^2(3) = 11.6, p = .008$  during threat conditioning resulted in models that significantly predicted BLA activity during immediate Transfer 2. Probing these interactions revealed that increased BLA PS+ (vs. PS-) during Transfer 2 was selectively related to the combined increased PS+ (vs. PS-) reactivation and increased univariate activity in hippocampus,  $\beta = 0.52, t_{wald}(53) = 2.43, p = .015, 95\%CI [.10, .95]$ , or mPFC,  $\beta = 0.45, t_{wald}(53) = 2.24, p = .025, 95\%CI [.06, .85]$ , during CS+ (vs. CS-) trials, confirming this effect as related to integrated aversive conditioning (see Fig. 5A).

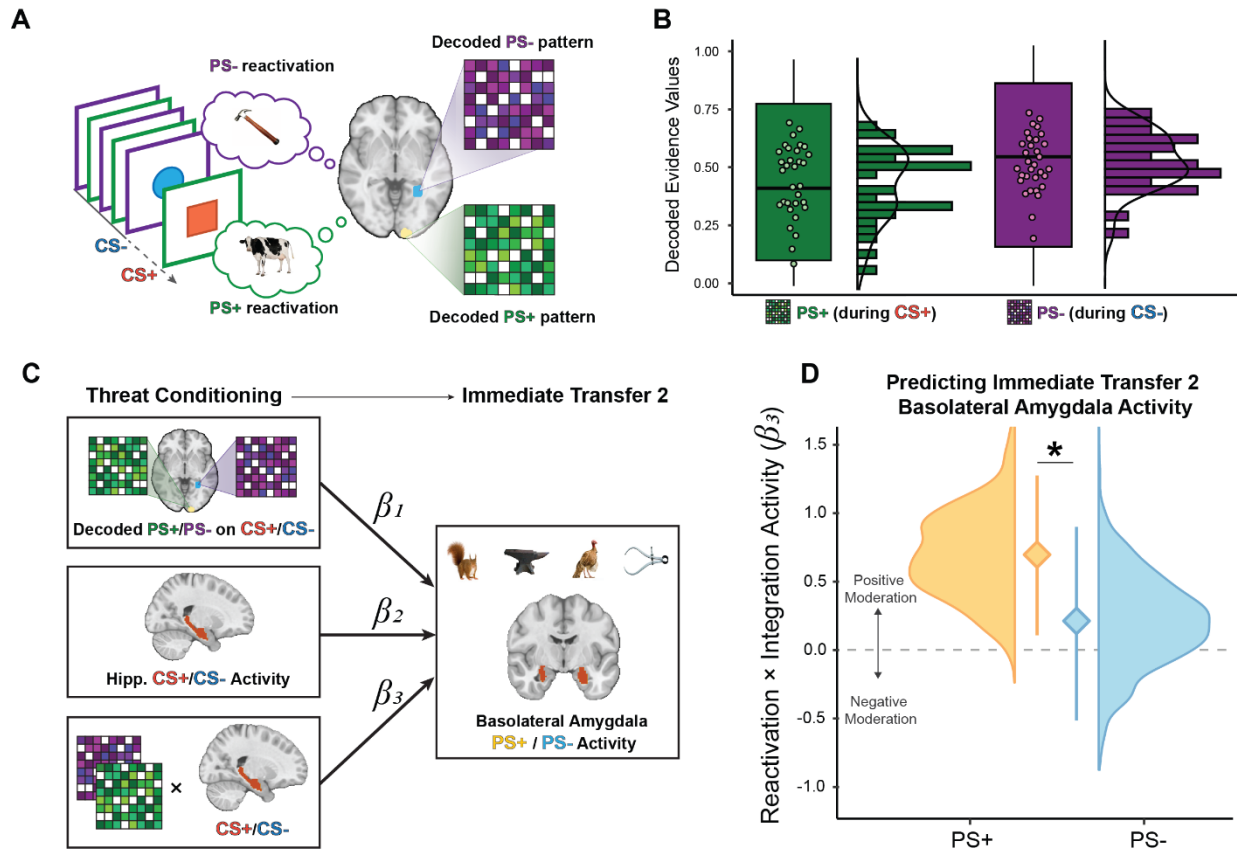


Fig 5. (A) Schematic of decoding analyses. During threat conditioning, PS reactivation is decoded using a machine learning classifier validated on localizer data. Decoding is conducted within functional localizer defined category-selective ROIs. Degree of reinstatement is indexed by evidence values reflecting the strength of the PS pattern. (B) Distribution of decoded PS+ and PS- evidence values. Distributions are indicative of sufficient variability for individual difference analyses. Mean evidence values for both PS+ and PS- are significantly different than zero (one-tailed  $t$ -test,  $p_s < .001$ ).

(C) Schematic of moderation analyses. Beta coefficients ( $\beta$ ) represent threat conditioning terms predicting the outcome variable (BLA activity during immediate Transfer 2).  $\beta_1$  represents the decoded PS during the CS from category-selective cortex,  $\beta_2$  represents univariate hippocampus activity during a CS, and  $\beta_3$  represents the interaction term between  $\beta_1$  and  $\beta_2$ . As lower-order terms modeled in an interaction are no longer interpretable as main effect

coefficients and are not interpreted in moderation analyses, they are included for model informational purposes only. The actual tested model is structured hierarchically, with all CS+/PS+ and CS-/PS+ data contained in multilevel stimulus term nested within each participant that was also interacted with the displayed lower-order and interaction coefficients. Interaction terms with this stimulus term are not visualized to streamline the depicted model.

(D) Cortical reactivation and online integration results. For visualization purposes, separate interaction coefficients (decoded PS reactivation x hippocampal CS activation) were extracted for Transfer 2 PS+ and PS- conditions and bootstrapped ( $k = 1000$ ). Coefficients, 95% confidence intervals, and distributions are plotted against zero to demonstrate significance. Positive coefficients with confidence intervals that do not contain (overlap) zero are significant positive moderators of the positive decoded PS reactivation x hippocampal CS activation interaction, such that the three-way interaction of these variables results in overall larger BLA activity during Transfer 2 for PS+, but not PS-, stimuli.

BLA = basolateral amygdala; CS+ = conditioned threat cue; CS- = conditioned safety cue; hipp. = hippocampus; PS+ = preconditioned threat cue; PS- = preconditioned safety cue.

\*  $p < .05$

## Discussion

The complexity of human experience necessitates a flexible memory system that can adapt to a range of novel experiences and efficiently update existing memories to reflect new information. Semantic networks, built up over multiple experiences, help facilitate this process by providing a scaffold for inference and behavioral selection, even without direct experience of potential consequences. Prior work implies that semantic structures could provide ingress points for learned threats to enter and then broadly generalize across semantic networks<sup>78–81</sup>. However, the mechanisms by which emotional experiences integrate with previously acquired semantic knowledge to modify the meaning and salience of different stimuli indirectly related to the experience have not been directly tested. The present study revealed potential mechanisms for building integrated memories of threat within a semantic network.

We showed that pre-association of a set of category exemplars with a to-be-conditioned stimulus modified the neural representation of unique category exemplars within category-selective occipitotemporal regions, the mPFC, and MTL regions that include the amygdala, hippocampus, and PRC. Specifically, pattern similarity amongst unique exemplars pre-associated with a threat cue became more similar following threat conditioning. Enhanced neural similarity could facilitate the transfer of emotional learning to a diverse set of category exemplars despite

their physical distinctions. This finding is consistent with a prior report of increased neural similarity in the occipitotemporal cortex and the amygdala for category-level stimuli directly predictive of an aversive US (direct conditioning)<sup>24</sup> but extends this finding to a higher-order learning paradigm (sensory preconditioning) that necessitates integrating across separate phases of learning. Modulation was transient in the occipitotemporal cortex and the amygdala but persisted beyond 24-hours in the hippocampus and PRC, suggesting separation between immediate and longer-term changes in neural organization among these regions.

Prior studies establish the PRC's role in storing semantic information<sup>82-84</sup>, and show that representational similarity covaries with semantic and visual dimensions<sup>85,86</sup>. Here, we observed modulation, from emotional learning, of stimulus representations in the PRC that persisted beyond 24-hours. The hippocampus also maintained increased within-category similarity for the indirectly threat-conditioned category, which is consistent with its central role in threat-related delayed recall and retrieval<sup>53,87,88</sup>. These findings extend reports of PRC and hippocampal involvement in sensory preconditioning<sup>14,19</sup> to demonstrate how the selectively modified representations extend beyond 24-hours following aversive learning.

At the moment of an emotional experience, do we immediately integrate this event with distinct past experiences to update related memories? Or does integration occur upon encountering a new situation that requires retrieval of the emotional memory? Prior research points to neither memory integration process as unilaterally superior nor predominant, such that both forms of integration can be involved when memory guides decision-making<sup>4,26,28</sup>. Our results suggest that humans employ both routes when integration involves modulation of pre-established semantic structures.

First, analysis of covert category reactivation during conditioning supports an online integration account: selective reactivation of a decoded indirectly conditioned category in occipitotemporal regions during threat conditioning interacted with increased hippocampal and mPFC activity to predict BLA activity during immediate transfer. Psychologically, this suggests retrieval of the pre-associated category representation is integrated into the newly formed threat memory at the moment of emotional learning. These decoding results align with prior neuroimaging work showing evidence of online integration of episodic memory<sup>17,89-92</sup>, as well as studies showing reactivated category-selective voxels predicting responses during a subsequent retrieval test in aversive learning<sup>87,93</sup> and associative inference tasks<sup>92,94</sup>. Hippocampal and mPFC involvement during integration that subserves later retrieval is central to prominent episodic memory models<sup>19,20,95</sup>. Here, the output of online integration between reactivation of a semantic category representation and activity in the hippocampus or mPFC at the moment of aversive conditioning was increased activity to novel presentations of the PS in the BLA, a prominent region in neural models describing emotion-episodic memory interactions<sup>96,97</sup>. Notably, decoded reactivation in occipitotemporal regions alone did not predict subsequent BLA activity; it was only through the interaction with hippocampal/mPFC activity at the moment of learning. This suggests an important role for regions critical to memory formation and retrieval that interact with semantic representations in higher-order visual cortex to promote future concept-based generalizations.

Alternatively, there is evidence of retrieval-based integration (i.e., chaining) from selective reinstatement of the threat-specific neural pattern during immediate transfer tests in the amygdala and mPFC. Specifically, overlapping fMRI patterns were selectively correlated with the formation of a threat memory on CS+ trials and retrieval of a threat memory on PS+ trials. One possibility is that the amygdala and mPFC play a more domain-general role in the retrieval of value information

at the time of retrieval. Reinstating CS+ specific patterns on PS+ trials could reflect the general affective salience of the PS+ cues following threat conditioning; the mPFC could support model-based inference<sup>27</sup> that helps evaluate unique instance of the PS category that were not directly encountered during pre-conditioning and thus lack a directly learned PS-CS association. Consequently, chaining in these regions could prioritize reinstatement of the CS-US relation to promote pattern completion and decrease threat discrimination between physically dissimilar category exemplars. Notably, reinstatement between threat memory formation and retrieval was not observed in category-selective visual cortex, hippocampus, or PRC, all components of the ventral visual stream specialized in object recognition<sup>98,99</sup> and regions yielding evidence of online integration, as detailed above. In this way, regions tuned towards object recognition and representation might facilitate memory integration through reactivation of previously encountered instances directly associated with the CS. Conversely, regions with a domain-general role in value-related information might reinstate the threat memory when the properties of a novel stimulus must be inferred from related but distinct past events.

Recognition memory was selectively (PS+ > PS-) and retroactively enhanced for items encoded prior to threat conditioning, in line with studies that tested direct threat conditioning of categories<sup>73,100</sup>. These results appear to be in line with accelerating research on behavioral tagging<sup>101,102</sup> of human episodic memory<sup>103</sup>. In short, this model proposes that a salient event can rescue weak memories formed minutes to hours before (or after) the salient event. Sensory preconditioning, per se, does not require a tag-and-capture mechanism, as there is no evidence to our knowledge that the time window between preconditioning and threat conditioning is a boundary condition for sensory preconditioning to be effective. However, the sensory preconditioning protocol could initiate a behavioral tagging mechanism, given the design involves

“weak” learning (PS-CS pairs) followed by a salient event (CS-US pairs). Here, the timing and overlapping events likely produced the retroactive memory benefit, which aligns with a recent study using a similar preconditioning design that found retroactive enhancement in relational episodic memory<sup>18</sup>. Notably, while the behavioral tagging model (based on the synaptic tag-and-capture model) is confined by the time window between the weak and strong event, other neurobiological models that are not constrained by this time boundary (co-allocation hypothesis;<sup>104–106</sup> could provide a neurobiological explanation for these retroactive memory results. It is noteworthy that the selective enhancement was not symmetrical; there was no proactive benefit on memory during transfer. The probe test might not have constituted a “weak” situation (in accordance with behavioral tagging phenomenon), as although participants did not explicitly expect shock, arousal was significantly elevated on typical PS+ items and neuroimaging results showed strong evidence of modulation of PS+ items during transfer within area formation areas. Finally, participants selectively rated items from the PS+ semantic category as more typical, in line with direct category-conditioning findings<sup>73</sup>. Memory integration appears to promote a more internally cohesive associative network whereby distinct category members are encoded as more representative of their superordinate category through indirect association with a threat cue.

Although physiological arousal during transfer was differentially affected by participants' ratings of category typicality, it is notable that physiological arousal was not maintained throughout the test, and participants overall did not expect shock to PS+ items. Desynchrony between threat measures is well-documented<sup>107,108</sup>, particularly between neural and behavioral or subjective outcomes<sup>109,110</sup>. Here, the lack of behavioral generalization might reflect an adaptive desynchrony: the brain encodes higher-order relationships and their threat salience, as this is relatively efficient and expends minimal resources. Meanwhile, overt behavioral responses are



enacted to most novel category stimuli because these stimuli are still quite unlikely to represent a genuine threat. The durability of our neural effects further supports this interpretation. Neural reorganization in response to the indirect threat conditioning was no longer present after 24-hours in the amygdala, mPFC, or occipitotemporal cortex, in contrast to the more long-lasting neural differences and associated behavioral expression seen in direct conditioning studies<sup>53,88,111</sup>.

The “strong situation” theory describes individual differences in threat learning as a function of experimental threat salience<sup>112,113</sup> and potentially explains our behavioral findings. Strong threat situations refer to tasks or contexts with sufficient biological salience to provoke a normative and undifferentiated response from most, resulting in near or complete zero variance in responding. In contrast, weak threat situations are those in which trait or state individual differences successfully predict responding because a clearly adaptive proscribed action is not required by the type or intensity of the encountered threat, leading to natural response variability. For example, most who see a honking truck about to hit them will step away to avoid severe harm, but when the truck is farther away, some people might attempt to quickly cross the road and others will wait to cross. Importantly, without sufficient between-person variation in a relevant candidate trait or psychopathology, a weak situation can become a strong (i.e., zero variability) situation. We propose that our sensory preconditioning protocol is a *de facto* weak situation for neural differences, but as the threat threshold for behavioral expression is elevated, it functions as a strong situation when testing those without threat-related psychopathology (e.g., PTSD).

The integration of emotional memories with existing knowledge is a pillar of human inference in a dynamic and sometimes dangerous world, but this process has received limited empirical attention. We used multivariate fMRI analyses to provide neurobehavioral explanations for the indirect integration of aversive learning with a pre-established semantic network. Evidence

for online and retrieval integration was dependent on neural region and analysis, supporting a “which-when” memory integration account<sup>28</sup> while suggesting next steps for further delineating the precise neural circuitry underlying these processes. However, after ~24 hours, canonical threat regions did not maintain threat-related neural representations and overall behavioral expression of threat learning was limited., which is possibly related to testing a psychiatrically healthy sample. PTSD is empirically related to increased threat-related neural activity at 24-hour recall<sup>114,115</sup> and PTSD symptomology is conceptually consistent with persistent higher-order threat learning<sup>116,117</sup>. As such, the current study provides a potentially potent tool for testing subtle pathogenic processes, as we expect that stronger ~24-hour reactivation and behavioral expression would emerge in relation to PTSD and potentially other anxiety-related psychopathology.

## References

1. Tolman, E. C. Cognitive maps in rats and men. *Psychological Review* **55**, 189–208 (1948).
2. Gewirtz, J. C. & Davis, M. Using Pavlovian Higher-Order Conditioning Paradigms to Investigate the Neural Substrates of Emotional Learning and Memory. *Learn. Mem.* **7**, 257–266 (2000).
3. Gostolupce, D., Lay, B. P. P., Maes, E. J. P. & Iordanova, M. D. Understanding Associative Learning Through Higher-Order Conditioning. *Frontiers in Behavioral Neuroscience* **16**, (2022).
4. Shohamy, D. & Daw, N. D. Integrating memories to guide decisions. *Current Opinion in Behavioral Sciences* **5**, 85–90 (2015).
5. Cooper, S. E. *et al.* A meta-analysis of conditioned fear generalization in anxiety-related disorders. *Neuropsychopharmacol.* **47**, 1652–1661 (2022).
6. Cooper, S. E. & Dunsmoor, J. E. Fear conditioning and extinction in obsessive-compulsive disorder: A systematic review. *Neuroscience & Biobehavioral Reviews* **129**, 75–94 (2021).
7. Fraunfelter, L., Gerdes, A. B. M. & Alpers, G. W. Fear one, fear them all: A Systematic Review and Meta-Analysis of Fear Generalization in Pathological Anxiety. *Neuroscience & Biobehavioral Reviews* 104707 (2022) doi:10.1016/j.neubiorev.2022.104707.
8. Zinbarg, R. E., Williams, A. L. & Mineka, S. A Current Learning Theory Approach to the Etiology and Course of Anxiety and Related Disorders. *Annu. Rev. Clin. Psychol.* (2022) doi:10.1146/annurev-clinpsy-072220-021010.
9. Ghosh, V. E. & Gilboa, A. What is a memory schema? A historical perspective on current neuroscience literature. *Neuropsychologia* **53**, 104–114 (2014).

10. Brogden, W. J. Sensory pre-conditioning. *Journal of Experimental Psychology* **25**, 323–332 (1939).
11. Brogden, W. J. Sensory preconditioning of human subjects. *Journal of Experimental Psychology* **37**, 527–539 (1947).
12. Rescorla, R. A. Simultaneous and successive associations in sensory preconditioning. *Journal of Experimental Psychology: Animal Behavior Processes* **6**, 207–216 (1980).
13. Rizley, R. C. & Rescorla, R. A. Associations in second-order conditioning and sensory preconditioning. *Journal of Comparative and Physiological Psychology* **81**, 1–11 (1972).
14. Holmes, N. M., Fam, J. P., Clemens, K. J., Laurent, V. & Westbrook, R. F. The neural substrates of higher-order conditioning: A review. *Neuroscience & Biobehavioral Reviews* **138**, 104687 (2022).
15. Holmes, N. M., Parkes, S. L., Killcross, A. S. & Westbrook, R. F. The Basolateral Amygdala Is Critical for Learning about Neutral Stimuli in the Presence of Danger, and the Perirhinal Cortex Is Critical in the Absence of Danger. *J. Neurosci.* **33**, 13112–13125 (2013).
16. Wong, F. S., Westbrook, R. F. & Holmes, N. M. ‘Online’ integration of sensory and fear memories in the rat medial temporal lobe. *eLife* **8**, e47085 (2019).
17. Wimmer, G. E. & Shohamy, D. Preference by Association: How Memory Mechanisms in the Hippocampus Bias Decisions. *Science* **338**, 270–273 (2012).
18. Zhu, Y. *et al.* Emotional learning retroactively promotes memory integration through rapid neural reactivation and reorganization. *eLife* **11**, e60190 (2022).
19. Schlichting, M. L. & Preston, A. R. Memory integration: neural mechanisms and implications for behavior. *Current Opinion in Behavioral Sciences* **1**, 1–8 (2015).

20. Zeithamova, D., Schlichting, M. L. & Preston, A. R. The hippocampus and inferential reasoning: building memories to navigate future decisions. *Front. Hum. Neurosci.* **6**, (2012).
21. Dunsmoor, J. E. & Murphy, G. L. Categories, concepts, and conditioning: how humans generalize fear. *Trends in Cognitive Sciences* **19**, 73–77 (2015).
22. Newell, F. N. *et al.* Multisensory perception constrains the formation of object categories: a review of evidence from sensory-driven and predictive processes on categorical decisions. *Philosophical Transactions of the Royal Society B: Biological Sciences* **378**, 20220342 (2023).
23. de Voogd, L. D., Fernández, G. & Hermans, E. J. Disentangling the roles of arousal and amygdala activation in emotional declarative memory. *Soc Cogn Affect Neurosci* **11**, 1471–1480 (2016).
24. Dunsmoor, J. E., Kragel, P. A., Martin, A. & LaBar, K. S. Aversive learning modulates cortical representations of object categories. *Cereb. Cortex* **24**, 2859–2872 (2014).
25. Morey, R. A. *et al.* Neural correlates of conceptual-level fear generalization in posttraumatic stress disorder. *Neuropsychopharmacol.* **45**, 1380–1389 (2020).
26. Biderman, N., Bakkour, A. & Shohamy, D. What Are Memories For? The Hippocampus Bridges Past Experience with Future Decisions. *Trends in Cognitive Sciences* **24**, 542–556 (2020).
27. Wang, F., Schoenbaum, G. & Kahnt, T. Interactions between human orbitofrontal cortex and hippocampus support model-based inference. *PLOS Biology* **18**, e3000578 (2020).

28. Holmes, N. M., Wong, F. S., Bouchekioua, Y. & Westbrook, R. F. Not “either-or” but “which-when”: A review of the evidence for integration in sensory preconditioning. *Neuroscience & Biobehavioral Reviews* **132**, 1197–1204 (2022).
29. Jones, P. J., Mair, P., Riemann, B. C., Mugno, B. L. & McNally, R. J. A network perspective on comorbid depression in adolescents with obsessive-compulsive disorder. *Journal of Anxiety Disorders* **53**, 1–8 (2018).
30. Sadacca, B. F. *et al.* Orbitofrontal neurons signal sensory associations underlying model-based inference in a sensory preconditioning task. *eLife* **7**, e30373 (2018).
31. Dunsmoor, J. E., White, A. J. & LaBar, K. S. Conceptual similarity promotes generalization of higher order fear learning. *Learn. Mem.* **18**, 156–160 (2011).
32. Tolin, D. F. *et al.* Psychometric Properties of a Structured Diagnostic Interview for DSM-5 Anxiety, Mood, and Obsessive-Compulsive and Related Disorders. *Assessment* **25**, 3–13 (2018).
33. Weathers, F. W. *et al.* The Clinician-Administered PTSD Scale for DSM–5 (CAPS-5): Development and Initial Psychometric Evaluation in Military Veterans. *Psychol Assess* **30**, 383–395 (2018).
34. Peirce, J. *et al.* PsychoPy2: Experiments in behavior made easy. *Behav Res* **51**, 195–203 (2019).
35. Bach, D. R. *et al.* Consensus design of a calibration experiment for human fear conditioning. *Neuroscience & Biobehavioral Reviews* **148**, 105146 (2023).
36. Hennings, A. C., Cooper, S. E., Lewis-Peacock, J. A. & Dunsmoor, J. E. Pattern analysis of neuroimaging data reveals novel insights on threat learning and extinction in humans. *Neuroscience & Biobehavioral Reviews* **142**, 104918 (2022).

37. Hennings, A. C., Bibb, S. A., Lewis-Peacock, J. A. & Dunsmoor, J. E. Thought suppression inhibits the generalization of fear extinction. *Behavioural Brain Research* **398**, 112931 (2021).
38. Cooper, S. E., Dunsmoor, J. E., Koval, K. A., Pino, E. R. & Steinman, S. A. Test–retest reliability of human threat conditioning and generalization across a 1-to-2-week interval. *Psychophysiology* **60**, e14242 (2023).
39. Green, S. R., Kragel, P. A., Fecteau, M. E. & LaBar, K. S. Development and validation of an unsupervised scoring system (Autonomate) for skin conductance response analysis. *International Journal of Psychophysiology* **91**, 186–193 (2014).
40. Lykken, D. T. & Venables, P. H. Direct Measurement of Skin Conductance: A Proposal for Standardization. *Psychophysiology* **8**, 656–672 (1971).
41. Lonsdorf, T. B. *et al.* Navigating the garden of forking paths for data exclusions in fear conditioning research. *eLife* **8**, e52465 (2019).
42. Esteban, O. *et al.* fMRIPrep: a robust preprocessing pipeline for functional MRI. *Nature Methods* **16**, (2019).
43. Fischl, B. FreeSurfer. *NeuroImage* **62**, 774–781 (2012).
44. Abraham, A. *et al.* Machine learning for neuroimaging with scikit-learn. *Frontiers in Neuroinformatics* **8**, (2014).
45. Mumford, J. A., Turner, B. O., Ashby, F. G. & Poldrack, R. A. Deconvolving BOLD activation in event-related designs for multivoxel pattern classification analyses. *NeuroImage* **59**, 2636–2643 (2012).
46. Mumford, J. A., Davis, T. & Poldrack, R. A. The impact of study design on pattern estimation for single-trial multivariate pattern analysis. *NeuroImage* **103**, 130–138 (2014).

47. Cox, R. W. AFNI: software for analysis and visualization of functional magnetic resonance neuroimages. *Comput Biomed Res* **29**, 162–173 (1996).
48. Fullana, M. A. *et al.* Neural signatures of human fear conditioning: an updated and extended meta-analysis of fMRI studies. *Mol Psychiatry* **21**, 500–508 (2016).
49. Yu, T., Lang, S., Birbaumer, N. & Kotchoubey, B. Neural correlates of sensory preconditioning: A preliminary fMRI investigation. *Human Brain Mapping* **35**, 1297–1304 (2014).
50. Amunts, K. *et al.* Cytoarchitectonic mapping of the human amygdala, hippocampal region and entorhinal cortex: intersubject variability and probability maps. *Anat Embryol* **210**, 343–352 (2005).
51. Ritchey, M., Montchal, M. E., Yonelinas, A. P. & Ranganath, C. Delay-dependent contributions of medial temporal lobe regions to episodic memory retrieval. *eLife* **4**, e05025 (2015).
52. Hennings, A. C., McClay, M., Lewis-Peacock, J. A. & Dunsmoor, J. E. Contextual reinstatement promotes extinction generalization in healthy adults but not PTSD. *Neuropsychologia* **147**, 107573 (2020).
53. Hennings, A. C., McClay, M., Drew, M. R., Lewis-Peacock, J. A. & Dunsmoor, J. E. Neural reinstatement reveals divided organization of fear and extinction memories in the human brain. *Current Biology* S096098222101527X (2022) doi:10.1016/j.cub.2021.11.004.
54. Kim, H., Smolker, H. R., Smith, L. L., Banich, M. T. & Lewis-Peacock, J. A. Changes to information in working memory depend on distinct removal operations. *Nat Commun* **11**, 6239 (2020).



55. Pedregosa, F. *et al.* Scikit-learn: Machine Learning in Python. *Journal of Machine Learning Research* **12**, 2825–2830 (2011).
56. Martin, A. The Representation of Object Concepts in the Brain. *Annu. Rev. Psychol.* **58**, 25–45 (2007).
57. R Core Team. R: A language and environment for statistical computing. (2018).
58. Chen, G., Saad, Z. S., Britton, J. C., Pine, D. S. & Cox, R. W. Linear mixed-effects modeling approach to fMRI group analysis. *NeuroImage* **73**, 176–190 (2013).
59. Chen, G. *et al.* Sources of Information Waste in Neuroimaging: Mishandling Structures, Thinking Dichotomously, and Over-Reducing Data. *Aperture Neuro* **2021**, (2022).
60. Field, A. P. & Wilcox, R. R. Robust statistical methods: A primer for clinical psychology and experimental psychopathology researchers. *Behaviour Research and Therapy* **98**, 19–38 (2017).
61. Koller, M. robustlmm: An R Package for Robust Estimation of Linear Mixed-Effects Models. *Journal of Statistical Software* **75**, 1–24 (2016).
62. Bates, D., Mächler, M., Bolker, B. & Walker, S. Fitting linear mixed-effects models using lme4. *Journal of Statistical Software* **67**, 1–51 (2015).
63. Lenth, R. V. emmeans: Estimated Marginal Means, aka Least-Squares Means. (2021).
64. Luke, S. G. Evaluating significance in linear mixed-effects models in R. *Behav Res* **49**, 1494–1502 (2017).
65. Arnqvist, G. Mixed Models Offer No Freedom from Degrees of Freedom. *Trends in Ecology & Evolution* **35**, 329–335 (2020).

66. Lüdtke, D., Ben-Shachar, M. S., Patil, I. & Makowski, D. parameters: Extracting, Computing and Exploring the Parameters of Statistical Models using R. *Journal of Open Source Software* **5**, 2445 (2020).
67. Rights, J. D., Preacher, K. J. & Cole, D. A. The danger of conflating level-specific effects of control variables when primary interest lies in level-2 effects. *British Journal of Mathematical and Statistical Psychology* **73**, 194–211 (2020).
68. Rights, J. D. & Sterba, S. K. On the Common but Problematic Specification of Conflated Random Slopes in Multilevel Models. *Multivariate Behavioral Research* 1–28 (2023) doi:10.1080/00273171.2023.2174490.
69. Yaremych, H. E., Preacher, K. J. & Hedeker, D. Centering categorical predictors in multilevel models: Best practices and interpretation. *Psychological Methods* **28**, 613–630 (2023).
70. Jiang, J., Wand, M. P. & Bhaskaran, A. Usable and Precise Asymptotics for Generalized Linear Mixed Model Analysis and Design. *Journal of the Royal Statistical Society Series B: Statistical Methodology* **84**, 55–82 (2022).
71. Li, P. & Redden, D. T. Comparing denominator degrees of freedom approximations for the generalized linear mixed model in analyzing binary outcome in small sample cluster-randomized trials. *BMC Medical Research Methodology* **15**, 38 (2015).
72. Dunsmoor, J. E. & Murphy, G. L. Stimulus typicality determines how broadly fear is generalized. *Psychological Science* **25**, 1816–1821 (2014).
73. Hennings, A. C., Lewis-Peacock, J. A. & Dunsmoor, J. E. Emotional learning retroactively enhances item memory but distorts source attribution. *Learn. Mem.* **28**, 178–186 (2021).

74. Keller, N. E., Hennings, A. C., Leiker, E. K., Lewis-Peacock, J. A. & Dunsmoor, J. E. Rewarded extinction increases amygdalar connectivity and stabilizes long-term memory traces in the vmPFC. *J. Neurosci.* JN-RM-0075-22 (2022) doi:10.1523/JNEUROSCI.0075-22.2022.
75. Reddan, M. C., Wager, T. D. & Schiller, D. Attenuating neural threat expression with imagination. *Neuron* **100**, 994-1005.e4 (2018).
76. Ritchey, M., Wing, E. A., LaBar, K. S. & Cabeza, R. Neural Similarity Between Encoding and Retrieval is Related to Memory Via Hippocampal Interactions. *Cerebral Cortex* **23**, 2818–2828 (2013).
77. Tompary, A. & Davachi, L. Consolidation Promotes the Emergence of Representational Overlap in the Hippocampus and Medial Prefrontal Cortex. *Neuron* **96**, 228-241.e5 (2017).
78. Bower, G. H. Mood and memory. *American Psychologist* **36**, 129–148 (1981).
79. Bower, G. H. How might emotions affect learning. *The handbook of emotion and memory: Research and theory* **3**, 31 (1992).
80. Foa, E. B. & Kozak, M. J. Emotional processing of fear: Exposure to corrective information. *Psychological Bulletin* **99**, 20–35 (1986).
81. Lang, P. J. Imagery in therapy: an information processing analysis of fear. *Behavior Therapy* **8**, 862–886 (1977).
82. Charest, I., Allen, E., Wu, Y., Naselaris, T. & Kay, K. Precise identification of semantic representations in the human brain. *Journal of Vision* **20**, 539 (2020).
83. Clarke, A. Dynamic activity patterns in the anterior temporal lobe represents object semantics. *Cognitive Neuroscience* **11**, 111–121 (2020).

84. Clarke, A. & Tyler, L. K. Object-Specific Semantic Coding in Human Perirhinal Cortex. *J. Neurosci.* **34**, 4766–4775 (2014).
85. Ferko, K. M. *et al.* Activity in perirhinal and entorhinal cortex predicts perceived visual similarities among category exemplars with highest precision. *eLife* **11**, e66884 (2022).
86. Martin, C. B., Douglas, D., Newsome, R. N., Man, L. L. & Barense, M. D. Integrative and distinctive coding of visual and conceptual object features in the ventral visual stream. *eLife* **7**, e31873 (2018).
87. Clewett, D., Dunsmoor, J., Bachman, S. L., Phelps, E. A. & Davachi, L. Survival of the salient: Aversive learning rescues otherwise forgettable memories via neural reactivation and post-encoding hippocampal connectivity. *Neurobiology of Learning and Memory* **187**, 107572 (2022).
88. Fullana, M. A. *et al.* Fear extinction in the human brain: A meta-analysis of fMRI studies in healthy participants. *Neuroscience & Biobehavioral Reviews* **88**, 16–25 (2018).
89. Richter, F. R., Chanals, A. J. H. & Kuhl, B. A. Predicting the integration of overlapping memories by decoding mnemonic processing states during learning. *NeuroImage* **124**, 323–335 (2016).
90. Shohamy, D. & Wagner, A. D. Integrating Memories in the Human Brain: Hippocampal–Midbrain Encoding of Overlapping Events. *Neuron* **60**, 378–389 (2008).
91. Zeithamova, D., Dominick, A. L. & Preston, A. R. Hippocampal and Ventral Medial Prefrontal Activation during Retrieval-Mediated Learning Supports Novel Inference. *Neuron* **75**, 168–179 (2012).
92. Zeithamova, D. & Preston, A. R. Temporal Proximity Promotes Integration of Overlapping Events. *Journal of Cognitive Neuroscience* **29**, 1311–1323 (2017).

93. de Voogd, L. D., Fernández, G. & Hermans, E. J. Awake reactivation of emotional memory traces through hippocampal–neocortical interactions. *NeuroImage* **134**, 563–572 (2016).
94. Mack, M. L. & Preston, A. R. Decisions about the past are guided by reinstatement of specific memories in the hippocampus and perirhinal cortex. *NeuroImage* **127**, 144–157 (2016).
95. Rugg, M. D. & Vilberg, K. L. Brain networks underlying episodic memory retrieval. *Current Opinion in Neurobiology* **23**, 255–260 (2013).
96. Dunsmoor, J. E. & Kroes, M. C. Episodic memory and Pavlovian conditioning: ships passing in the night. *Current Opinion in Behavioral Sciences* **26**, 32–39 (2019).
97. Gagnon, S. A. & Wagner, A. D. Acute stress and episodic memory retrieval: neurobiological mechanisms and behavioral consequences. *Annals of the New York Academy of Sciences* **1369**, 55–75 (2016).
98. Kanwisher, N. Neural events and perceptual awareness. *Cognition* **79**, 89–113 (2001).
99. Turk-Browne, N. B. The hippocampus as a visual area organized by space and time: A spatiotemporal similarity hypothesis. *Vision Research* **165**, 123–130 (2019).
100. Dunsmoor, J. E., Murty, V. P., Davachi, L. & Phelps, E. A. Emotional learning selectively and retroactively strengthens memories for related events. *Nature* **520**, 345–348 (2015).
101. Ballarini, F., Moncada, D., Martinez, M. C., Alen, N. & Viola, H. Behavioral tagging is a general mechanism of long-term memory formation. *Proceedings of the National Academy of Sciences* **106**, 14599–14604 (2009).
102. de Carvalho Myskiw, J., Benetti, F. & Izquierdo, I. Behavioral tagging of extinction learning. *Proceedings of the National Academy of Sciences* **110**, 1071–1076 (2013).

103. Dunsmoor, J. E., Murty, V. P., Clewett, D., Phelps, E. A. & Davachi, L. Tag and capture: how salient experiences target and rescue nearby events in memory. *Trends in Cognitive Sciences* (2022) doi:10.1016/j.tics.2022.06.009.
104. Cai, D. J. *et al.* A shared neural ensemble links distinct contextual memories encoded close in time. *Nature* **534**, 115–118 (2016).
105. Rashid, A. J. *et al.* Competition between engrams influences fear memory formation and recall. *Science* **353**, 383–387 (2016).
106. Rogerson, T. *et al.* Synaptic tagging during memory allocation. *Nat Rev Neurosci* **15**, 157–169 (2014).
107. Boddez, Y. *et al.* Rating data are underrated: Validity of US expectancy in human fear conditioning. *Journal of Behavior Therapy and Experimental Psychiatry* **44**, 201–206 (2013).
108. Rachman, S. & Hodgson, R. I. Synchrony and desynchrony in fear and avoidance. *Behaviour Research and Therapy* **12**, 311–318 (1974).
109. LeDoux, J. E. & Hofmann, S. G. The subjective experience of emotion: a fearful view. *Current Opinion in Behavioral Sciences* **19**, 67–72 (2018).
110. LeDoux, J. E. & Pine, D. S. Using Neuroscience to Help Understand Fear and Anxiety: A Two-System Framework. *AJP appi.ajp.2016.16030353* (2016) doi:10.1176/appi.ajp.2016.16030353.
111. Visser, R. M., Scholte, H. S., Beemsterboer, T. & Kindt, M. Neural pattern similarity predicts long-term fear memory. *Nature Neuroscience* **16**, 388–390 (2013).
112. Beckers, T., Krypotos, A.-M., Boddez, Y., Effting, M. & Kindt, M. What's wrong with fear conditioning? *Biological Psychology* **92**, 90–96 (2013).

113. Lissek, S., Pine, D. S. & Grillon, C. The strong situation: A potential impediment to studying the psychobiology and pharmacology of anxiety disorders. *Biological Psychology* **72**, 265–270 (2006).
114. Lissek, S. & van Meurs, B. Learning models of PTSD: Theoretical accounts and psychobiological evidence. *International Journal of Psychophysiology* (2014)  
doi:10.1016/j.ijpsycho.2014.11.006.
115. Suarez-Jimenez, B. *et al.* Neural signatures of conditioning, extinction learning, and extinction recall in posttraumatic stress disorder: a meta-analysis of functional magnetic resonance imaging studies. *Psychological Medicine* 1–10 (2019)  
doi:10.1017/S0033291719001387.
116. Dunsmoor, J. E., Cisler, J. M., Fonzo, G. A., Creech, S. K. & Nemeroff, C. B. Laboratory models of post-traumatic stress disorder: The elusive bridge to translation. *Neuron* (2022)  
doi:10.1016/j.neuron.2022.03.001.
117. Keane, T. M., Zimering, R. T., Caddell, J. M., & others. A behavioral formulation of posttraumatic stress disorder in Vietnam veterans. *Behavior Therapist* **8**, 9–12 (1985).

### **Acknowledgments**

The authors would like to thank Ayesha Nadiadwala, Ryan Webler, Nicole Keller, and Josh Cisler for helpful discussions and comments regarding analyses and conceptual framework.

S.E.C. is funded by the NIH (F32 MH129136). J.A.L.-P. is funded by the NIH (R01 EY028746 and R01 MH129042). J.E.D. is funded by the NIH (R01 MH122387) and the NSF (CAREER Award 1844792).